

Supporting Information

Evaluation of triphenylene-based MOF ultrathin films for lithium batteries

Isabel Ciria-Ramos^{a,b}, Inés Tejedor^{a,b}, Lucía Caparros, Beatriz Doñagueda, Oscar Lacruz, Ainhoa Urtizberea^{a,c}, Olivier Roubeau^a, Ignacio Gascón^{a,b}, Marta Haro^{a,b*}

^a Instituto de Nanociencia y Materiales de Aragón (INMA), CSIC-Universidad de Zaragoza, Zaragoza, 50009, Spain

^b Departamento de Química Física, Facultad de Ciencias, Universidad de Zaragoza, Plaza San Francisco, Zaragoza, 50009, Spain

^c Departamento de Ciencia y Tecnología de Materiales y Fluidos, EINA, Universidad de Zaragoza, Zaragoza, 50018, Spain

* mharo@unizar.es

Contents

Surface pressure decay vs time while barriers are stopped in <i>cssc</i> protocol	2
Surface potential rise vs time during barriers are stopped in <i>cssc</i> protocol	2
Model of the 2D Ni ₃ (HHTP) ₂ planes	3
UV-vis reflection spectra of the Ni ₃ (HHTP) ₂ Langmuir film using the <i>cc</i> protocol	3
AFM images of Cu foil substrate	4
Cyclic Voltammetry at different ν rates	4
Estimation of b-value	5
CV plots at 0.1 mVs ⁻¹ before and after cycling	5
High resolution XPS spectra of C1s and O1s	6

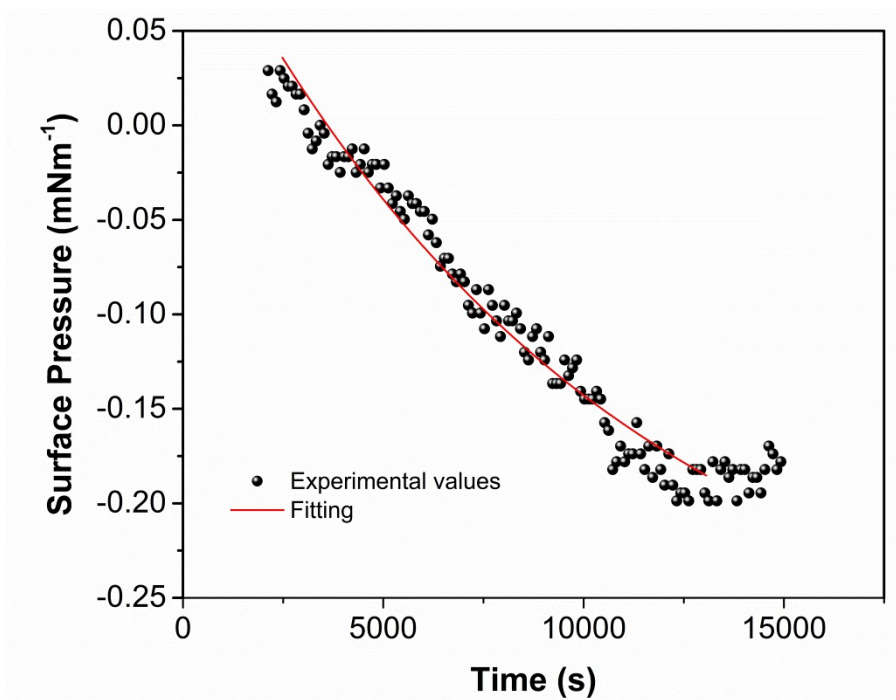


Figure SI.1. Surface Pressure vs time during while the barriers are stopped in the *cssc* protocol and the fitted plot (red line): $\pi=0.45\exp(-t/10183)-0.306$ ($R^2=0.97$), where the kinetic constant is $9.8 \cdot 10^{-5} \text{ s}^{-1}$.

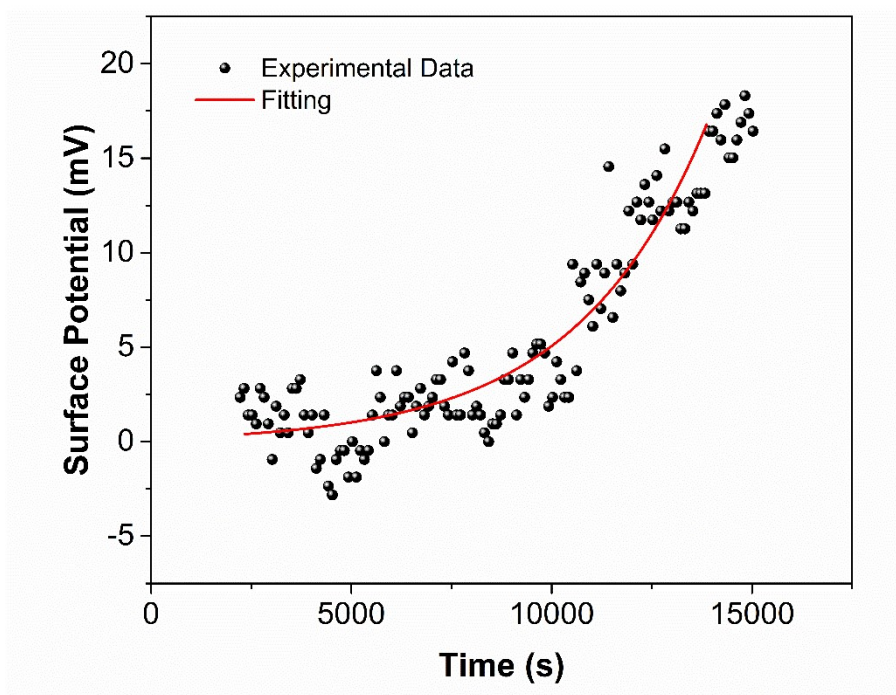


Figure SI.2. Surface Potential vs time during the barriers are stopped in the *cssc* protocol and the fitted plot (red line): $\Delta V=0.24\exp(t/3261)-0.09$ ($R^2=0.87$), where the kinetic constant is $3.1 \cdot 10^{-4} \text{ s}^{-1}$.

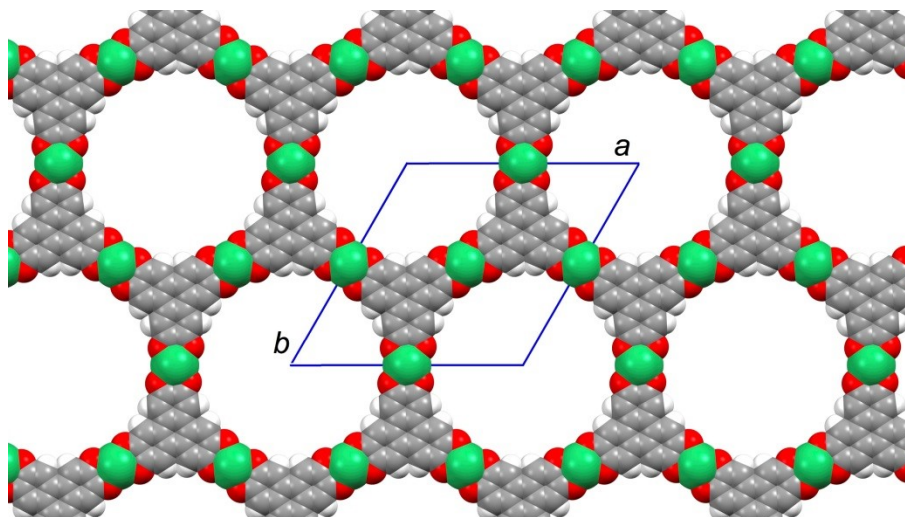


Figure SI.3. View of the structural model of the 2D $\text{Ni}_3(\text{HHTP})_2$ planes based on the structure of the bulk material which contains in addition intercalated layers of $\text{Ni}_3(\text{HOTP})(\text{H}_2\text{O})_6$ ¹. The model uses a lower symmetry hexagonal space group $P6$ and $a = b = 23.25 \text{ \AA}$. The slightly expanded cell parameters with respect to the 22.13 \AA for the bulk material is a likely consequence of the flattening of the whole 2D structure in the same plane.

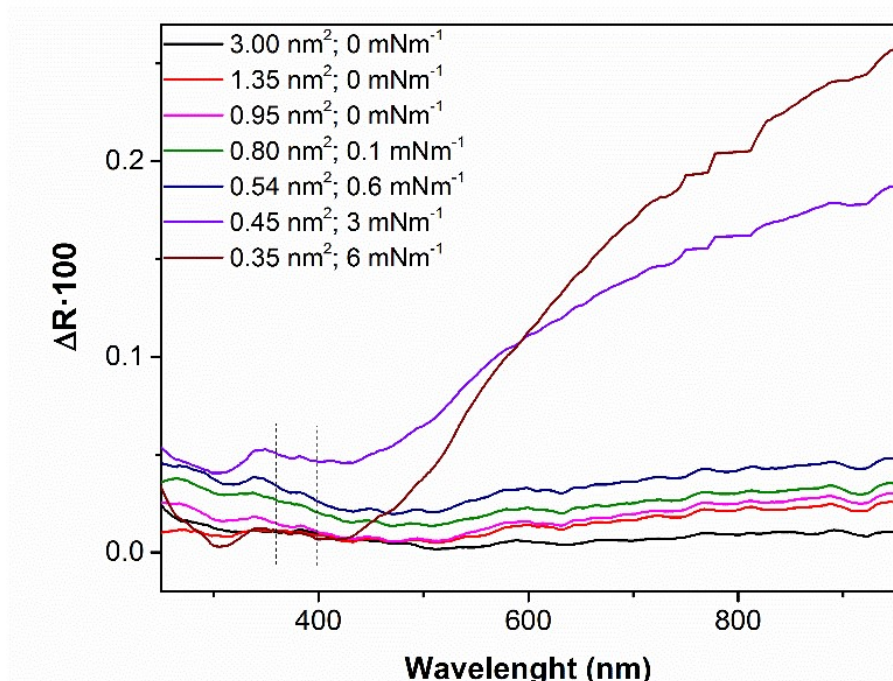


Figure SI.4. Reflection UV-vis spectra of $\text{Ni}_3(\text{HHTP})_2$ Langmuir films at different areas per HHTP during compression process with cc protocol.

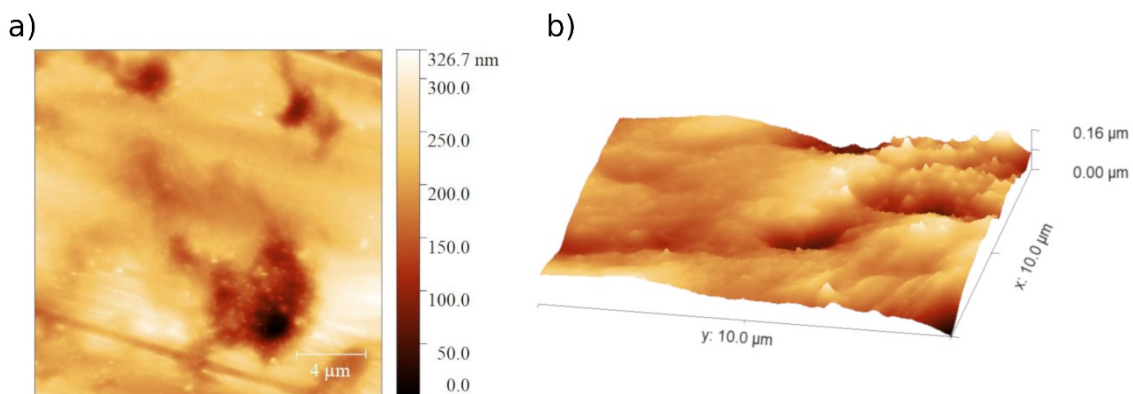


Figure SI.5. AFM images of bare Cu foil used as substrate for the $\text{Ni}_3(\text{HHTP})_2$ LS electrodes. The images show defects in the order of hundred nanometers.

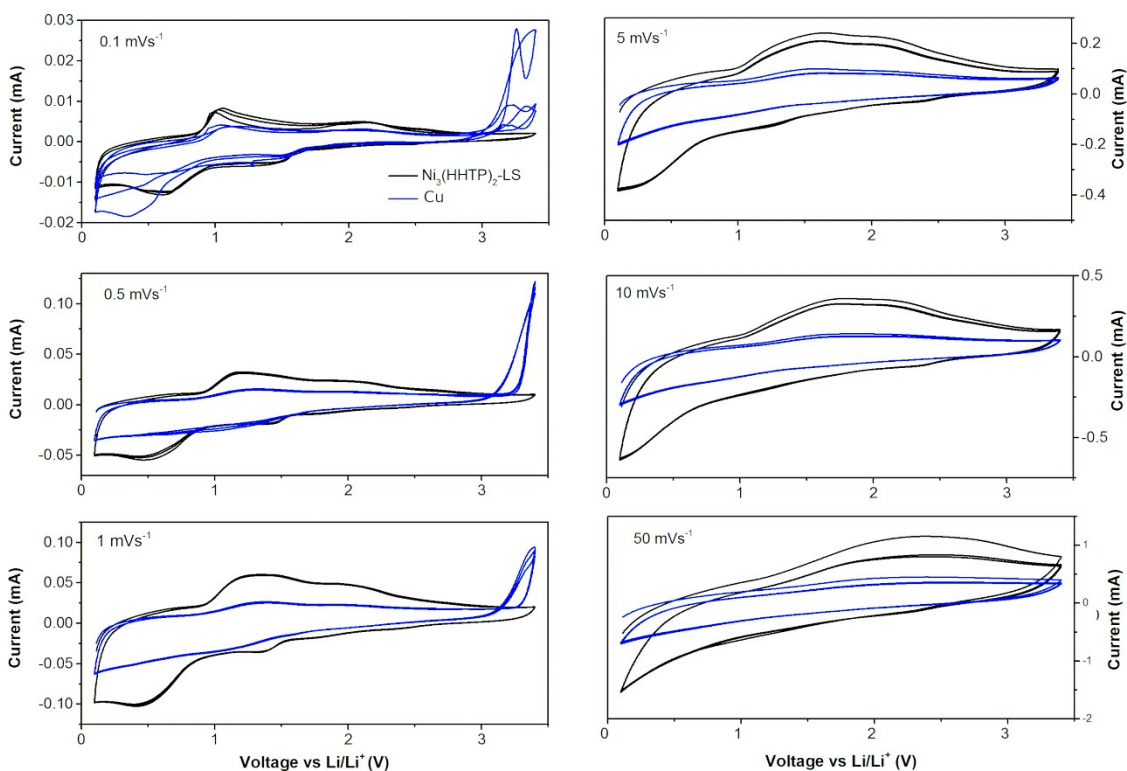


Figure SI.6. 3 CV cycles of a Li semibattery using Cu foil bare (blue line) or covered with a LS film of 20 transferences of $\text{Ni}_3(\text{HHTP})_2$ (black line) at the indicated sweep speed. The first cathodic sweep where the SEI is formed is not represented.

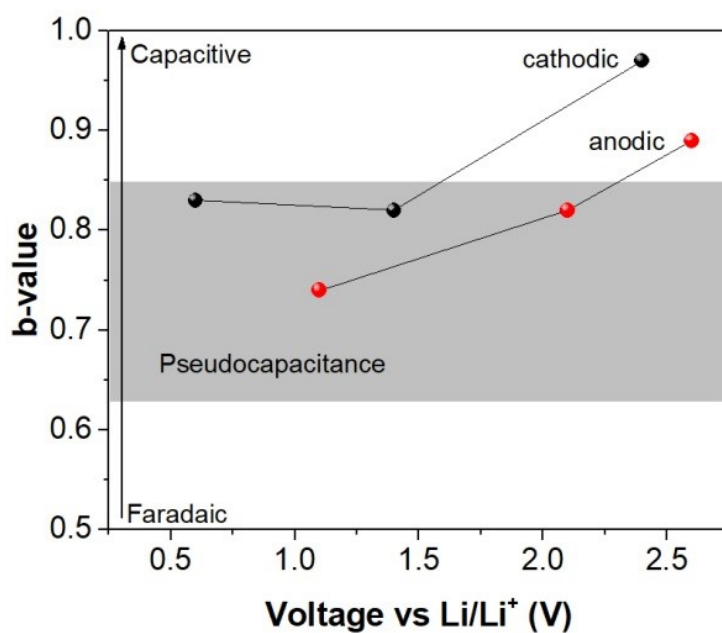


Figure SI.7. b-value calculated for cssc-20t electrode from the CV performed at 0.5 mVs⁻¹.

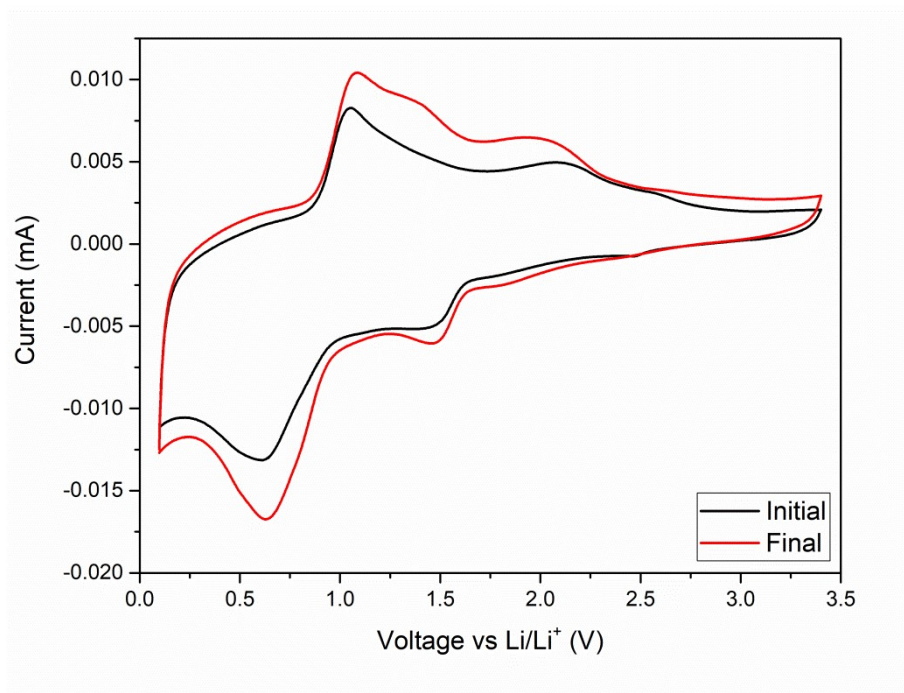


Figure SI.8. CV plots of Ni₃(HHTP)₂ LS films and lithium batteries at 0.1 mVs⁻¹, in the first third cycle (black) and in the last cycle (red) after performing 3 CV cycles at the different rates of 0.5 mVs⁻¹, 1 mVs⁻¹, 5 mVs⁻¹, 10 mVs⁻¹, and 50 mVs⁻¹. The absence of new peaks and the similar current density of both plots indicate good stability of the LS films without the appearance of new species or new regions of uncovered Cu substrate for detachment of the LS film.

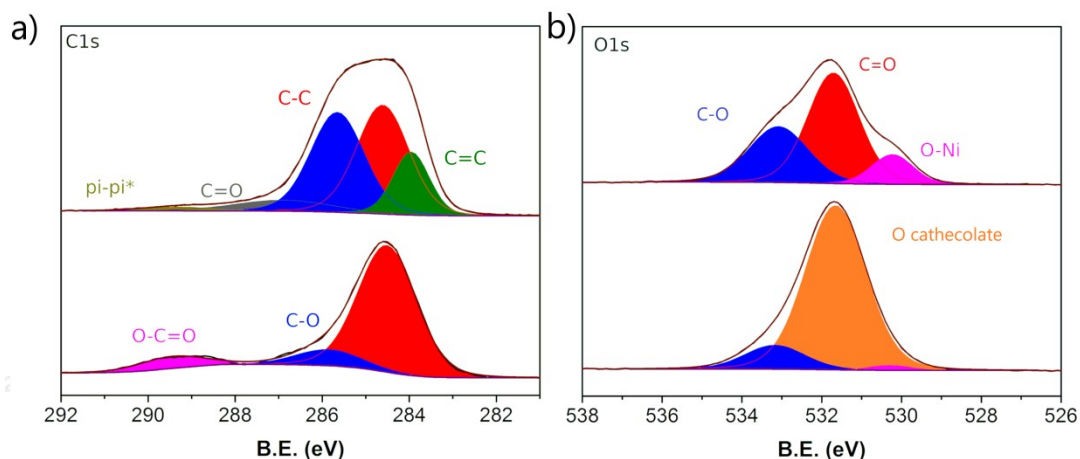


Figure SI.9. High resolution XPS spectra of: **a)** C 1s, and **b)** O 1s for pristine $\text{Ni}_3(\text{HHTP})_2$ LS film (top) and after being cycled as electrode in Li-semibattery at disassembled when the voltage was 0.1 V vs Li/Li⁺ (bottom).

The C 1s high resolution spectrum for the pristine sample can be deconvoluted in three main components related to C-C (or C-H), C=C and C-O, and two minor ones attributed to C=O and pi-pi* stacking². In the cycled sample, the main peak related to C 1s appears at 284.5 eV, peak related to C-C, and the peak C-O in reduced band. This is an unexpected result, and it can be due to the detection of the polymer formed in the SEI³, which hinders the detection of C=C and C-O components of the subjacent MOF film. This hypothesis is supported with the apparition of a new peak at 289.0 eV, attributable to the presence of O=C-O which is part of the SEI (solid electrolyte interface)⁴. It is also possible the contribution of Li_xC_6 specie, which shows the C 1s peak at 285.2 eV and the Li 1s at 57 eV⁵, although these peaks are also reported at 282 eV and 52 eV⁶, respectively. The O 1s high resolution spectrum (Figure 6d) can be fitted with three components, attributed to the quinone (C=O), semiquinone (C-O) configurations and to O-Ni⁷. This assignment is a bit controversial, and it can also be assigned to H₂O, oxygen linked to carbon (C-O or C=O) and O-Ni². After cycling, the O 1s spectrum conforms mainly to the peak associated with the catecholate configuration, indicating the accumulation of negative charge on this atom in the presence of lithium ions. However, part of the contribution to the band at ~531.5 eV can be also due to the ether carbon formed in the SEI³, in accordance to the C 1s high resolution XPS spectrum.

References

1. M. Hmadeh, Z. Lu, Z. Liu, F. Gándara, H. Furukawa, S. Wan, V. Augustyn, R. Chang, L. Liao and F. Zhou, *Chem. Mater.*, 2012, **24**, 3511-3513.
2. H. Wu, W. Zhang, S. Kandambeth, O. Shekhah, M. Eddaoudi and H. N. Alshareef, *Advanced Energy Materials*, 2019, **9**, 1900482.
3. D. Enslin, M. Stjerndahl, A. Nyén, T. Gustafsson and J. O. Thomas, *Journal of Materials Chemistry*, 2009, **19**, 82-88.
4. S. Leroy, H. Martinez, R. Dedryvère, D. Lemordant and D. Gonbeau, *Appl. Surf. Sci.*, 2007, **253**, 4895-4905.
5. G. Wertheim, P. T. M. Van Attekum and S. Basu, *Solid State Commun.*, 1980, **33**, 1127-1130.
6. K. Ciosek Högström, S. Malmgren, M. Hahlin, H. Rensmo, F. Thébault, P. Johansson and K. Edstrom, *The Journal of Physical Chemistry C*, 2013, **117**, 23476-23486.
7. J. Sun, L. Guo, X. Sun, J. Zhang, Y. Liu, L. Hou and C. Yuan, *Journal of Materials Chemistry A*, 2019, **7**, 24788-24791.